



Design and development of a new functionalized cellulose-based magnetic nanocomposite: preparation, characterization, and catalytic application in the synthesis of diverse pyrano[2,3-*c*]pyrazole derivatives

Ali Maleki¹ · Vahid Eskandarpour¹

Received: 7 July 2018 / Accepted: 23 January 2019 / Published online: 7 February 2019
© Iranian Chemical Society 2019

Abstract

In this work, a facile protocol for the preparation of a new cellulose-based functionalized magnetic nanocomposite catalyst is described. The structure and morphology of the prepared nanomaterial was characterized by scanning electron microscopy, energy-dispersive X-ray analysis, X-ray diffraction patterns, and Fourier transform infrared spectroscopy analyses. Then, its catalytic activity was investigated in the synthesis of 2,4-dihydropyrano[2,3-*c*]pyrazole and spiro[indoline-3,4'-pyrano[2,3-*c*]pyrazole derivatives through a one-pot four-component reaction between isatin or aldehydes or acetophenones, ethylacetate, hydrazine hydrate, and malononitrile or ethylcyanoacetate in short reaction times, high yields, and mild conditions. The nanocomposite was simply separated by an external magnet and reused several times without remarkable loss of activity.

Keywords Cellulose composite · Magnetic bionanostructure · Heterogeneous nanocatalyst · Spiroindoline · Pyranopyrazoles

Introduction

Multicomponent reactions (MCRs) are an important tool to efficiently synthesis of various complex molecules in one-pot conditions starting from at least three simple and readily available raw materials. In the recent years, researchers have increased their interest in MCRs and used this strategy for pharmaceutical and drug discovery research [1, 2].

One of the most important challenges in pharmaceutical chemistry is the synthesis of biologically active molecules via economical protocols [3]. Dihydropyrano[2,3-*c*]pyrazoles play an important role in the synthesis of biologically active compounds. These compounds have many properties such as antimicrobial [4], insecticidal [5], and anti-inflammatory activities [6].

In the synthesis of pyranopyrazoles, three-component (3-CR) or four-component (4-CR) reactions are often

used [7–11]. In the 4-CR, carbonyl compounds, hydrazine hydrate, β -keto-ester, and malononitrile condensed in the presence of a catalyst. Different catalysts have been reported for these reactions such as tetraethylammonium [12], $[(\text{CH}_2)_4\text{SO}_3\text{HMIM}][\text{HSO}_4]$ [13] and Al_2O_3 [14].

The indole moiety is one of the most important heterocycles which is involved in a variety of natural products and medicinal agents [15–19]. Compounds carrying the indole moiety exhibit antibacterial and antifungal activities [15–19]. Furthermore, it has been reported that C-3 spiroindoline derivatives highly enhance biological activity of chemical compounds [16–19].

Most of the reported protocols for the synthesis of both these products, especially in the case of spiroindoline–pyranopyrazoles, were suffering from disadvantages such as expensive reagents, long reaction times, low yields, toxic reagents, and harsh reaction conditions. Hence, development of an effective method for the synthesis of these scaffolds is significant. The preparation of an efficient catalyst is also necessary. In the past decade, functionalized magnetic catalysts have been the center of attentions due to their diverse advantages such as a broad range of applications, reusability, high stability, availability, and easy

✉ Ali Maleki
maleki@iust.ac.ir

¹ Catalysts and Organic Synthesis Research Laboratory, Department of Chemistry, Iran University of Science and Technology, Tehran 16846-13114, Iran

separation [20]. As a result, nanocatalysts are reliable and a promising option for chemists to be utilized in organic reactions.

In the past decades, functionalized magnetic catalysts have been the center of attention due to their diverse advantages such as a broad range of application, reusability, high stability, availability, and easy separation [21]. In connection with our previous works on the introduction of novel protocols in MCRs and bionanostructure catalysts [22–26], herein, the preparation and characterization of γ -Fe₂O₃@cellulose-OSO₃H as a new bionanocomposite that catalyzes the effective synthesis of 2,4-dihydropyrano[2,3-*c*]pyrazole (Fig. 1, path A) and spiro[indoline-3,4'-pyrano[2,3-*c*]pyrazole] (Fig. 1, path B) at room temperature are described. This nanocatalyst can remove simply after completion of the reaction by an external magnetic field.

Reported methods hint different disadvantages, such as expensive reagents, long reaction times, low yields, and use of the toxic reagents in both of the reactions, especially, for spiroindoline–pyranopyrazoles production. Therefore, the use of effective catalysts will be an important approach to reduce these issues.

Results and discussion

Catalyst characterization

Initially, γ -Fe₂O₃ nanoparticles were synthesized by coprecipitation method using cellulose microcrystals. As indicated in Fig. 2, the size and morphology of the nanoparticles were studied by scanning electron microscopy (SEM). SEM images proved the homogeneous structure of the catalyst. The cellulose layer was coated homogeneously on the

surface of the nanoparticles. The average size of nanoparticles was about 25–55 nm.

Figure 3 shows the Fourier transform infrared (FT-IR) spectra of γ -Fe₂O₃@cellulose-OSO₃H in comparison with cellulose and cellulose-OSO₃H. A broad band at 3350 cm⁻¹ was observed which is attributed to $\sigma_{\text{O-H}}$ stretching vibrations of OH groups on cellulose structure that due to the structure of each spectrum, the substrate cellulose nanocomposite structure proved to be designed. Hydrogen bonding is the reason of the broadness of this band. Due to the presence of nanoparticles between hydrogen bonds in the cellulose or cellulose-OSO₃H structure, the OH band of the nanocomposite is lower than them. In the IR spectrum of nanocomposite, a new band at 437 cm⁻¹ is related to Fe–O bonds in Fe₂O₃ nanoparticles that can prove the nanoparticle synthesis on cellulose surface. In addition, the decrease in the height of OH broadband also is another reason for why Fe₂O₃ nanoparticles have been placed on the cellulose surface. Other important bands, which must be appeared at 580 and 634 cm⁻¹, are not distinguished because of overlapping with cellulose bands. The stretching vibrations of S=O bands should have been seen at 1032 cm⁻¹ related to SO₃H is not seen due to the overlapping with cellulose bands located at 1046 cm⁻¹.

To determine the elements composition in the nanocomposite structure, the γ -Fe₂O₃@cellulose-OSO₃H was analyzed by energy-dispersive X-ray (EDX) analysis. As shown in Fig. 4, elements C, O, F, and S were indicated. Cellulosic surface structure confirms the elements C and O as well as Fe and O in the synthesis of nanoparticles on the surface. In addition, existence of SO₃H groups on the nanocomposite structure was confirmed by sulfur element on this analysis.

X-ray powder diffraction (XRD) pattern was also used to determine the structure of the nanocatalyst. The XRD

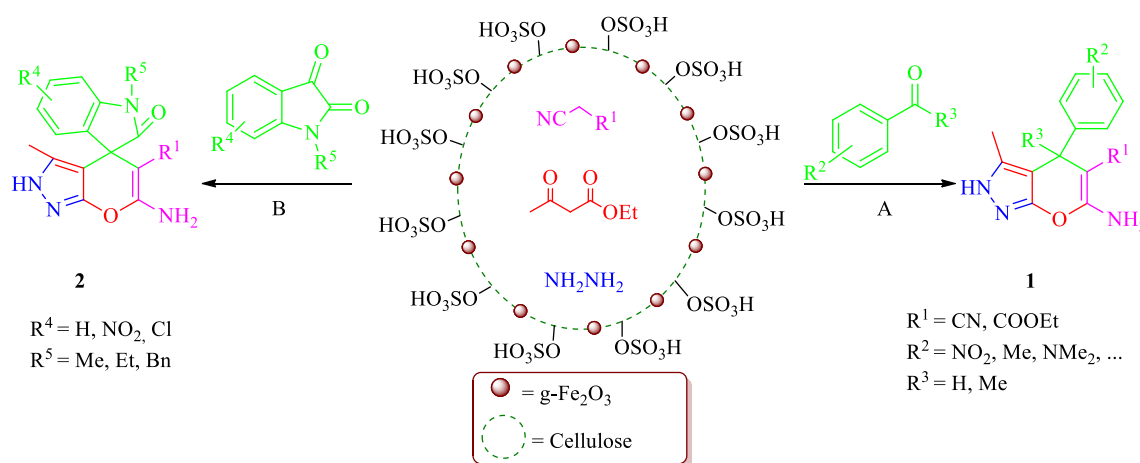


Fig. 1 Synthesis of 2,4-dihydropyrano[2,3-*c*]pyrazoles **1** and spiro[indoline-3,4'-pyrano[2,3-*c*]pyrazole] derivatives **2** through four-component reactions of isatin or aldehyde or acetophenone

derivatives, malononitrile or ethylcyanoacetate, ethyl acetoacetate and hydrazine hydrate catalyzed by γ -Fe₂O₃@cellulose-OSO₃H

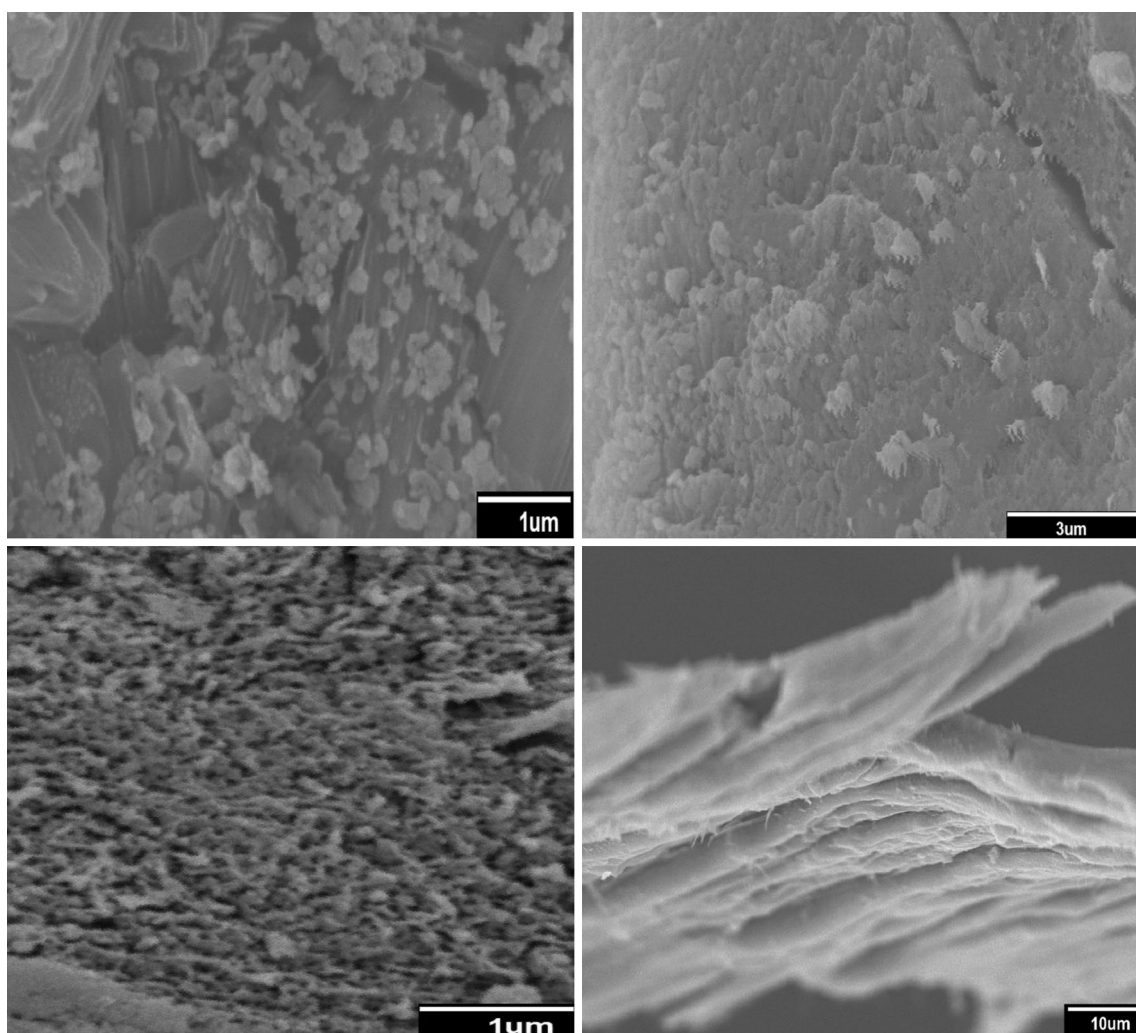


Fig. 2 SEM images of $\gamma\text{-Fe}_2\text{O}_3$ @cellulose-OSO₃H showing the layered structure of cellulose with $\gamma\text{-Fe}_2\text{O}_3$ nanoparticles on its surface in different magnifications

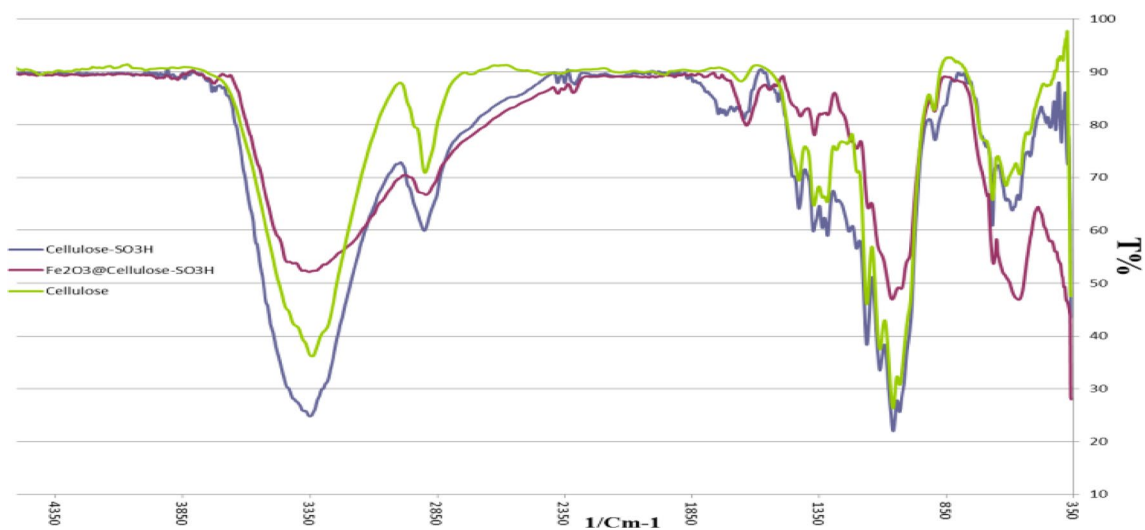


Fig. 3 FT-IR spectra of the $\gamma\text{-Fe}_2\text{O}_3$ @cellulose-OSO₃H in comparison with cellulose and cellulose-OSO₃H

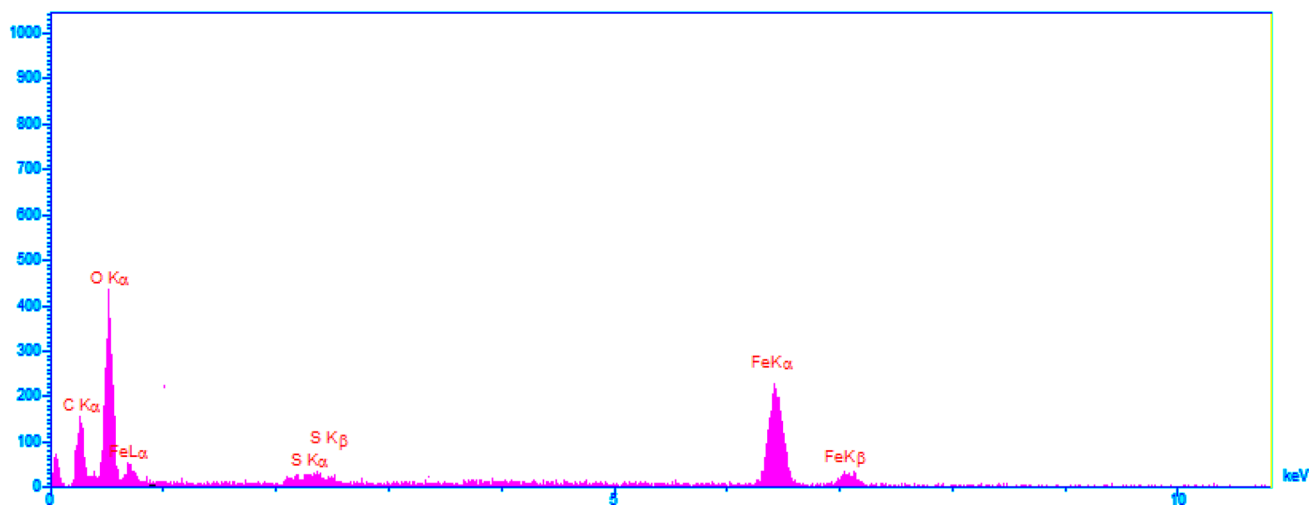


Fig. 4 EDX analysis of the $\gamma\text{-Fe}_2\text{O}_3$ @cellulose- OSO_3H nanocatalyst

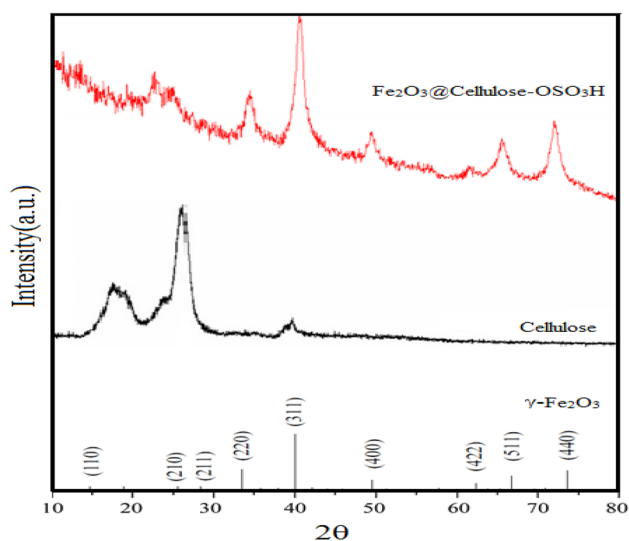


Fig. 5 XRD pattern of $\gamma\text{-Fe}_2\text{O}_3$ @cellulose- OSO_3H , cellulose, and $\gamma\text{-Fe}_2\text{O}_3$

pattern of the $\gamma\text{-Fe}_2\text{O}_3$ @cellulose- OSO_3H nanocomposite is shown in Fig. 5. The peak in region $2\theta = 20$ degree, which is a curved peak, represents the cellulose substrate and cellulose XRD. The sharp peaks in the region of $30\text{--}65^\circ$ are related to $\gamma\text{-Fe}_2\text{O}_3$ nanoparticles on its surface. This could easily be proven by comparing with the $\gamma\text{-Fe}_2\text{O}_3$ pattern. The XRD pattern of the $\gamma\text{-Fe}_2\text{O}_3$, along with its relationship with the crystalline planes of each signal, corresponds perfectly with nanocomposite crystalline signals. These results showed that $\gamma\text{-Fe}_2\text{O}_3$ @cellulose- OSO_3H has been successfully synthesized. The $\gamma\text{-Fe}_2\text{O}_3$ peaks at XRD pattern are as follows: 2 2 0, 3 3 1, 4 0 0, 4 2 2, 5 1 1, and 4 4 0. The XRD pattern peaks of the obtained nanocomposite are as

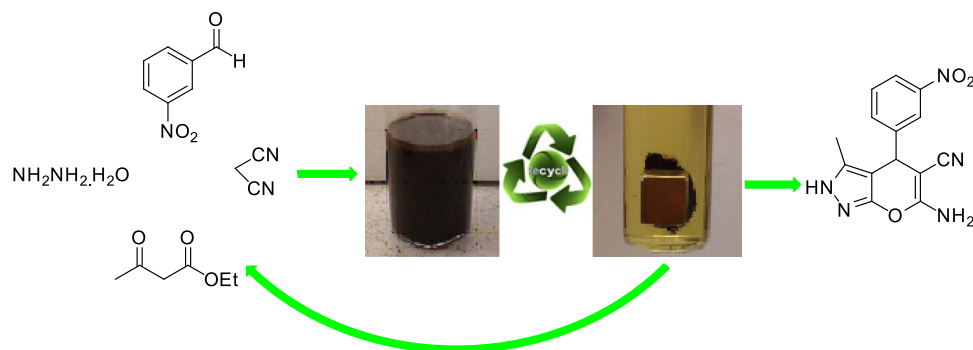
follows: $2\theta = 30.3^\circ, 35.8^\circ, 43.35^\circ, 53.7^\circ, 57.3^\circ,$ and 62.91° and XRD pattern of cellulose fibers shows two peaks at $2\theta = 22.7^\circ$ and 16.7° . According to the above results, it can be figured out that the patterns resulted from $\gamma\text{-Fe}_2\text{O}_3$ @cellulose- OSO_3H nanocomposite was in accordance with cellulose and $\gamma\text{-Fe}_2\text{O}_3$ patterns. This confirms the synthesis of $\gamma\text{-Fe}_2\text{O}_3$ nanoparticles inside cellulose sulfuric acid matrix. The average size of the nanoparticles is about 32 nm which is obtained via Scherrer equation:

$$d = \frac{K\lambda}{\beta \cos \theta}$$

Inspection of the catalytic activity of $\gamma\text{-Fe}_2\text{O}_3$ @cellulose- OSO_3H in the synthesis of pyranopyrazole and spiro-indole-pyranopyrazole derivatives

Synthesis of pyranopyrazole compounds using $\gamma\text{-Fe}_2\text{O}_3$ @cellulose- OSO_3H as catalyst

To optimize the reaction conditions, we considered the reaction of 3-nitrobenzaldehyde, ethylacetoacetate, malononitrile, and hydrazine hydrate (molar ratios of 1:1:1:1) as a model reaction (Fig. 6). First, this reaction was attempted under catalyst-free conditions, but after 1 h, the product was obtained in low yield. Therefore, the presence of catalyst for completion of this reaction is necessary. A number of catalysts such as Al_2O_3 , [14] tetraethylammonium bromide [12], $[(\text{CH}_2)_4\text{SO}_3\text{HMIM}][\text{HSO}_4]$ [13], and meglumine [37] were reported. Some of these catalysts need heating at refluxing and provide low yields after long reaction times. In comparison with those catalysts, new nanocomposite ($\gamma\text{-Fe}_2\text{O}_3$ @cellulose- OSO_3H) proved to be the most efficient one which gave higher yield (96%) in 3 min with a very small amount

Fig. 6 Model reaction of the pyranopyrazole synthesis**Table 1** Screening of γ -Fe₂O₃@cellulose-OSO₃H and solvent effects on the model reaction

Entry	Solvent	Catalyst amount (g)	Time (min)	Yield ^a (%)
1	Ethanol	–	60	trace
2	Ethanol	0.001	3	70
3	Ethanol	0.005	3	96
4	Ethanol	0.01	3	96
5	Ethanol	0.02	3	97
6	Ethanol	0.025	3	97
7	Water	0.005	3	80
8	Acetonitrile	0.005	3	90
9	Chloroform	0.005	3	70

^aReaction conditions: 1 mmol of 3-nitrobenzaldehyde, 1 mmol of ethyl acetoacetate, 1 mmol malononitrile and 1 mmol of hydrazine hydrate

of catalyst. The results are shown in Table 1. The progress of the reaction was monitored by TLC. In summary, the reaction time and yield of model reaction at room temperature and ethanol as a solvent in the presence of 0.005 g nanocatalyst were the best condition. Therefore, some other pyranopyrazole derivatives were synthesized with aforementioned mole ratio and in optimized condition utilized from the model reaction. These results persuaded us to other carbonyl compounds (aldehyde, acetophenone, and malononitrile derivatives (malononitrile or ethylcyanoacetate) for the synthesis of pyranopyrazole compounds. This reaction has the advantages of easy separation of catalyst by an external magnet, use of acetophenone derivatives, the first report of using ethylcyanoacetate instead of malononitrile, high yield and short reaction time, excellent recyclability of catalyst, use of the eco-friendly solvent, and easy workup.

We investigated aldehydes and acetophenones containing both electron-withdrawing and electron-donating groups and also malonitrile derivatives (malononitrile and ethylcyanoacetate). Due to very short reaction time in aldehyde derivatives, effects of these groups are not comprehensible and in reactivity of acetophenones, steric hindrance effects of groups are not salient, either. However, in case of acetophenones,

compounds which contain electron-withdrawing groups react better and require short reaction time when compared to those containing of electron-donating groups. Because of the presence of methyl group in acetophenones and steric hindrance of this group, reaction time with acetophenone is longer than aldehydes. In the case of malononitrile derivatives (malononitrile or ethylcyanoacetate), no differences were observed in reaction time.

Table 2 clearly shows that the reaction of various aromatic aldehydes or acetophenones, malononitrile, ethyl acetoacetate, and hydrazine hydrate in ethanol as a solvent and the nanocomposite provided the corresponding pyranopyrazole in high yields and short reaction time. Some of these derivatives were produced for the first time, and for ensure of formation of them, these compounds were analyzed with melting point, IR, and NMR spectral data.

To show the efficiency of γ -Fe₂O₃@cellulose-OSO₃H as appropriate catalyst for pyranopyrazole synthesis, we compared our results with other results which have been reported using various catalysts in Table 3. To compare the catalytic activity of γ -Fe₂O₃ nanoparticles or SO₃H, cellulose sulfuric acid and γ -Fe₂O₃@cellulose were synthesized and applied in model reaction. The results showed, in the presence both these catalysts, that reaction time was longer and reaction yield was lower. However, in the presence of this new nanocomposite [with Lewis acid (γ -Fe₂O₃) and Brønsted–Lowry acid (SO₃H)], the results were better.

Synthesis of spiro[indoline-3,4'-pyrano[2,3-c]pyrazole] derivatives using γ -Fe₂O₃@cellulose-OSO₃H

To optimize the reaction conditions, we considered the reaction of isatin, ethylacetoacetate, malononitrile, and hydrazine hydrate (mole ratios 1:1:1:1) as a model reaction (Table 4). The progress of the reaction was monitored by TLC. According to results that were showed in this table, because of trace yield of spiro[indoline-3,4'-pyrano[2,3-c]pyrazole], the presence of catalyst is necessary for the effective reaction progress and gaining high yield. A few reports observed for this reaction. Triethanolamine, meglumine, piperidine, 4-DMAP, and NaBr/electricity passed (F/mol)

Table 2 Synthesis of pyranopyrazole derivatives using $\gamma\text{-Fe}_2\text{O}_3\text{@cellulose-OSO}_3\text{H}$

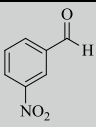
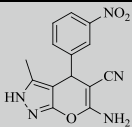
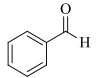
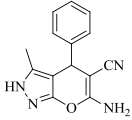
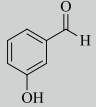
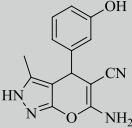
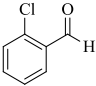
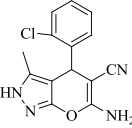
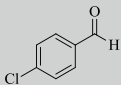
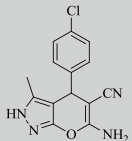
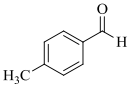
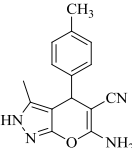
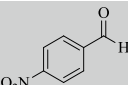
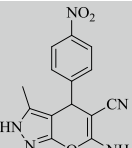
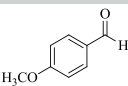
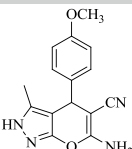
Entry	Aldehyde	CH-acid	Product	Time (min)	Yield ^a (%)	Mp (°C)	Mp (°C, refs)
1		NC-CH ₂ -CN		3	96	244–246	250–252 [16, 17, 18, 19]
2		NC-CH ₂ -CN		2	92	226–228	214–216 [27]
3		NC-CH ₂ -CN		4	86	241–243	233–235 [31]
4		NC-CH ₂ -CN		4	95	244–245	245 [30]
5		NC-CH ₂ -CN		3	84	176–178	178–180 [16, 17, 18, 19]
6		NC-CH ₂ -CN		4	95	184–186	175–177 [20]
7		NC-CH ₂ -CN		2	96	249–251	250 [20]
8		NC-CH ₂ -CN		4	89	198–199	208–209 [16, 17, 18, 19]

Table 2 (continued)

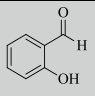
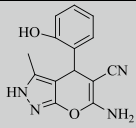
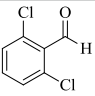
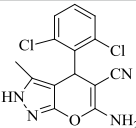
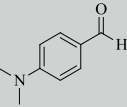
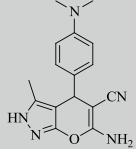
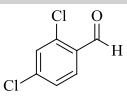
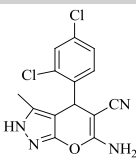
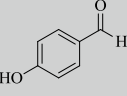
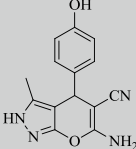
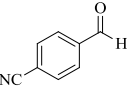
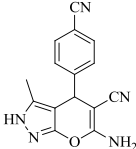
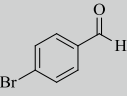
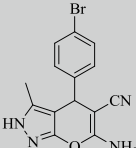
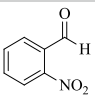
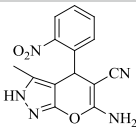
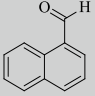
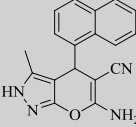
9		<chem>NC#CC#N</chem>		4	89	184–186	184–186 [28]
10		<chem>NC#CC#N</chem>		4	90	218–220	188–190 [27]
11		<chem>NC#CC#N</chem>		3	94	211–213	220 [30]
12		<chem>NC#CC#N</chem>		3	98	198–199	196–198 [27]
13		<chem>NC#CC#N</chem>		3	95	217–218	222–224 [29]
14		<chem>NC#CC#N</chem>		2	96	235	196–198 [16, 17, 18, 19]
15		<chem>NC#CC#N</chem>		2	99	200–201	181–183 [20]
16		<chem>NC#CC#N</chem>		3	92	227–228	223–224 [32]
17		<chem>NC#CC#N</chem>		3	94	218–219	200–202 [21]

Table 2 (continued)

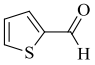
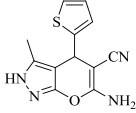
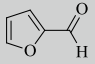
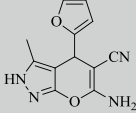
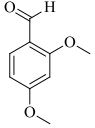
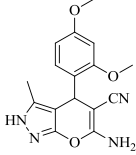
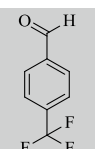

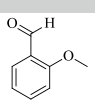
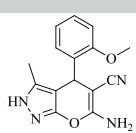
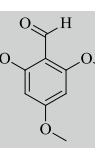
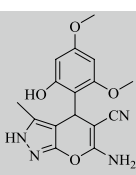
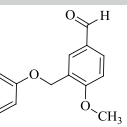
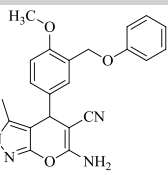
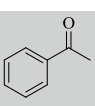
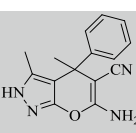
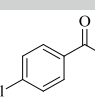
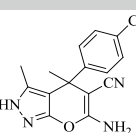
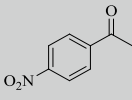
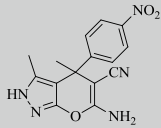
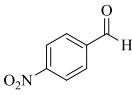
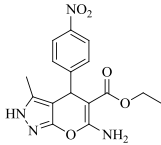
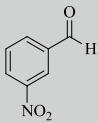
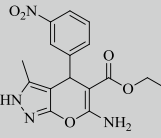
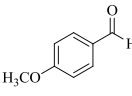
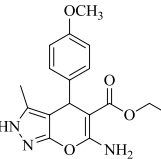
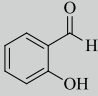
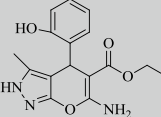
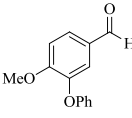
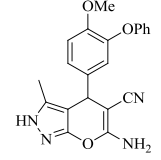
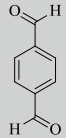
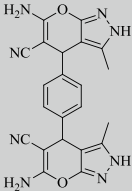
18		<chem>NC#CC#N</chem>		4	88	190–192	190–191 [32]
19		<chem>NC#CC#N</chem>		3	93	238–230	218–220 [27]
20		<chem>NC#CC#N</chem>		3	99	184–186	222–224 [27]
21		<chem>NC#CC#N</chem>		3	99	219	244–245 [33]
22		<chem>NC#CC#N</chem>		4	98	244	250 [30]
23		<chem>NC#CC#N</chem>		3	99	238.5– 239.5	Not reported
24		<chem>NC#CC#N</chem>		3	94	189–191	189–191 [34]
25		<chem>NC#CC#N</chem>		7	88	174–176	174–175 [32]
26		<chem>NC#CC#N</chem>		8	89	220–221	181–183 [28]

Table 2 (continued)

27		<chem>NC#CC#N</chem>		6	94	193–195	Not reported
28		<chem>NC#CC(=O)OCC</chem>		2	90	244–246	Not reported
29		<chem>NC#CC(=O)OCC</chem>		3	90	156–158	Not reported
30		<chem>NC#CC(=O)OCC</chem>		4	88	166–168	130 [41]
31		<chem>NC#CC(=O)OCC</chem>		4	88	153–154	143 [41]
32		<chem>NC#CC#N</chem>		3	91	189–191	Not reported
33		<chem>NC#CC#N</chem>		3	95	> 300	300 [40]

^aReaction conditions: aldehyde or acetophenone (1 mmol), malononitrile or ethylcyanoacetate (1 mmol), ethyl acetoacetate (1 mmol), hydrazine hydrate (1 mmol) and 0.005 g γ -Fe₂O₃@cellulose-OSO₃H, room temperature, 2 mL ethanol

are some of catalysts applied for this reaction. Almost all of these catalysts were used once, so they do not have reusability in organic synthesis and organocatalysts, such as piperidine, are poison, too. Some of these catalysts need difficult conditions such as electricity passed, ultrasonic, high temperature, or low yields in long reaction time. Hence, a new catalyst that eliminates these problems is necessary.

γ -Fe₂O₃@cellulose-OSO₃H is effective and catalyzed this reaction in high yield and low reaction time and its separation from reaction pot, by an external magnetic field is very simple. In the pilot reaction, according to the results that showed conditions, the efficiency and yields of the products in ethanol as a green solvent at room temperature were higher than other solvent. 0.01 g of the catalyst was

Table 3 Comparison of the catalytic efficiency of $\gamma\text{-Fe}_2\text{O}_3\text{@cellulose-OSO}_3\text{H}$ with other catalysts for the synthesis 2,4-dihydropyrano[2,3-*c*]pyrazoles

Entry	Catalyst	Catalyst amount	Conditions	Time (min)	Yield (%)
1	Tetraethylammonium bromide [12]	1 mmol	H ₂ O/reflux	10–30	68–90
2	[(CH ₂) ₄ SO ₃ HMIM][HSO ₄] [13]	1 mmol	Solvent-free/r.t	30	85–90
3	Al ₂ O ₃ [14]	0.5 mol%	H ₂ O/reflux	35–60	70–90
4	Fe ₂ O ₃ @cellulose	0.005 g	EtOH/r.t	60	60–65
5	Cellulose sulfuric acid	0.005 g	EtOH/r.t	60	70–73
6	Fe ₂ O ₃ @cellulose-OSO ₃ H	0.005 g	EtOH/r.t	2–3	84–99

Table 4 Screening of $\gamma\text{-Fe}_2\text{O}_3\text{@cellulose-OSO}_3\text{H}$ and solvent effects for the synthesis of 6'-amino-3'-methyl-2-oxo-2'H-spiro[indoline-3,4'-pyrano[2,3-*c*]pyrazole]-5'-carbonitrile

Entry	Solvent	Catalyst amount (g)	Time (min)	Yield ^a (%)
1	Ethanol	–	120	–
2	Ethanol	0.005	40	80
3	Ethanol	0.01	40	93
4	Ethanol	0.02	40	93
5	Ethanol	0.025	40	88
6	Water	0.01	40	–
7	Acetonitrile	0.01	40	–
8	Chloroform	0.01	40	–

^aReaction conditions: 1 mmol of isatin, 1 mmol of ethylacetoacetate, 1 mmol malononitrile, and 1 mmol of hydrazine hydrate

an optimized amount of the catalyst for this reaction. More or lower amounts of catalyst decrease the yield in the same reaction time.

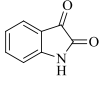
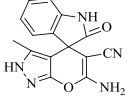
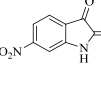
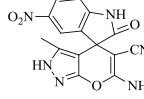
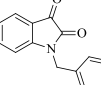
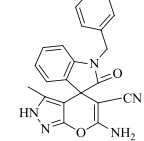
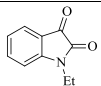
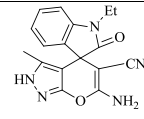
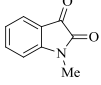
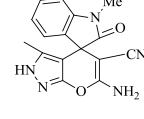
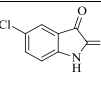
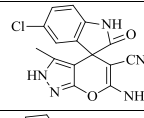
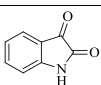
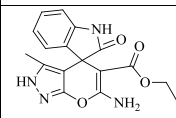
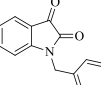
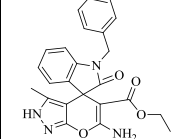
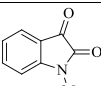
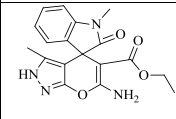
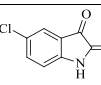
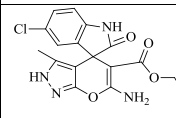
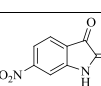
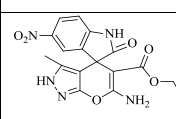
Then, we decided to develop this optimized conditions to other isatins and ethylcyanoacetate as a malononitrile derivative for the synthesis of spiro[indoline-3,4'-pyrano[2,3-*c*]pyrazole] derivatives (Table 5). We investigated isatins containing NO₂ or Cl on benzene ring and N–R derivatives of isatins. According to results that are listed in Table 5, in the presence of electron-withdrawing groups on the benzene of isatin, its chemical activity increases but with larger group on nitrogen of isatin, its activity decreases. In general, isatins which contain electron-withdrawing groups require shorter reaction time in comparison with those with N–R derivatives of isatin. This is also related to steric hindrance effects of alkyl groups.

To develop the optimized conditions, other isatins and ethylcyanoacetate as a malononitrile derivative were used for the synthesis of spiro[indoline-3,4'-pyrano[2,3-*c*]pyrazole] derivatives. According to results shown in Table 5, isatins which contain electron-withdrawing groups require shorter reaction times than those with N–R derivative of isatin. This may also be related to steric hindrance effects of alkyl groups.

To show the ability of $\gamma\text{-Fe}_2\text{O}_3\text{@cellulose-OSO}_3\text{H}$ as a useful catalyst for the synthesis of spiro[indoline-3,4'-pyrano[2,3-*c*]pyrazole] derivatives through one-pot four-component reaction, we compared our outcomes with other results which has been reported using various catalysts under different conditions (Table 6).

To investigate the recoverability and reusability of $\gamma\text{-Fe}_2\text{O}_3\text{@cellulose-OSO}_3\text{H}$ catalyst, it was tested in the reaction of 3-nitrobenzaldehyde, ethylacetoacetate, malononitrile, and hydrazine hydrate (mole ratio 1:1:1:1) and isatin, ethylacetoacetate, malononitrile, and hydrazine hydrate (mole ratio 1:1:1:1) as pilot reactions. After

Table 5 Synthesis of spiro[indoline-3,4'-pyrano[2,3-c]pyrazole] derivatives using γ -Fe₂O₃@cellulose-OSO₃H

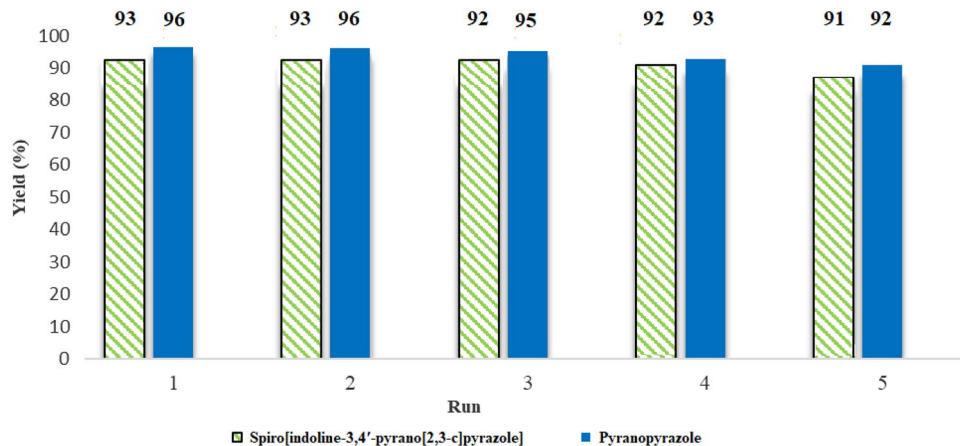
Entry	Isatin	CH-acid	Product	Time (min)	Yield (%) ^a	Mp (°C)	Mp (°C, refs)
1		NC-CH ₂ -CN		40	93	294–295	285–286 [35]
2		NC-CH ₂ -CN		35	95	270–271	270 [39]
3		NC-CH ₂ -CN		42	94	218–222	210 [36]
4		NC-CH ₂ -CN		42	94	180–182	176–178 [39]
5		NC-CH ₂ -CN		42	93	268–269	270–272 [35]
6		NC-CH ₂ -CN		35	93	296–297	297–298 [35]
7		NC-CH ₂ -COOEt		42	92	180	170–172 [36]
8		NC-CH ₂ -COOEt		48	92	133–135	125–128 [36]
9		NC-CH ₂ -COOEt		45	89	183–185	180–182 [39]
10		NC-CH ₂ -COOEt		40	92	280–282	Not reported
11		NC-CH ₂ -COOEt		40	91	265	Not reported

^aReaction conditions: isatin derivatives (1 mmol), malononitrile or ethyl cyanoacetate (1 mmol), ethyl acetoacetate (1 mmol), hydrazine hydrate (1 mmol), 0.01 g of γ -Fe₂O₃@cellulose-OSO₃H, room temperature, 2 mL of EtOH

Table 6 Comparison of the catalytic efficiency of $\gamma\text{-Fe}_2\text{O}_3\text{@cellulose-OSO}_3\text{H}$ with other catalysts for the synthesis of spiro[indoline-3,4'-pyrano[2,3-c]pyrazole]

Entry	Catalyst	Amount of catalyst	Reaction conditions	Time (min)	Yield (%)
1	Triethanolamine [36]	20 mmol	EtOH/reflux	120	43–68
2	Meglumine [37]	10 mol%	EtOH:H ₂ O/r.t	25–40	85–93
3	Piperidine [39]	10 mol%	H ₂ O/r.t	300	80–97
4	4-DAP [38]	10 mol%	EtOH/60 °C	60	75–87
5	Piperidine [25]	50 mg	EtOH/ultrasonic	60	69–93
6	NaBr [38]	0.01 g	EtOH/electricity	64	51–98
7	$\gamma\text{-Fe}_2\text{O}_3\text{@cellulose-OSO}_3\text{H}$	0.01 g	EtOH r.t	30–42	89–95

Fig. 7 Examination of $\gamma\text{-Fe}_2\text{O}_3/\text{Cu@cellulose}$ reusability in the synthesis of 6'-amino-3'-methyl-2-oxo-2'H-spiro[indoline-3,4'-pyrano[2,3-c]pyrazole]-5'-carbonitrile and 6-amino-3-methyl-4-(3-nitrophenyl)-2,4-dihydropyrano[2,3-c]pyrazole-5-carbonitrile



completion of the reaction, the nanocatalyst was simply separated by an external magnet. Then washed with hot ethanol and dried at room temperature. The catalyst was used and recycled five times without significant loss of activity (Fig. 7).

Conclusions

In summary, a new protocol was developed for the preparation of $\gamma\text{-Fe}_2\text{O}_3\text{@cellulose-OSO}_3\text{H}$ bionanostructure catalyst. The structure and morphology of the prepared nanocomposite were well confirmed by SEM, EDX, XRD, and FT-IR analyses. Then, its catalytic activity was investigated in two important syntheses of pyranopyrazoles and spiroindoline–pyranopyrazoles. This nanocomposite was easily separated by an external magnet and was effective reusable at least five times without remarkable loss of catalytic activity. The syntheses of pyranopyrazoles and spiroindoline–pyranopyrazoles were carried out through one-pot four-component reactions between isatin or aromatic aldehyde or acetophenone derivatives, ethylacetoacetate, hydrazine hydrate, and malononitrile or ethylcyanoacetate. This protocol had many advantages such as short reaction times, high yields, mild reaction conditions, and low requirement of the catalyst amount.

Experimental section

General

All solvents, chemicals, and reagents were purchased from Merck or Aldrich and used as received. Melting points were determined using an Electrothermal 9100 apparatus. FT-IR spectra were recorded as KBr pellets on a Shimadzu FT-IR-8400S spectrometer. Analytical TLC was carried out using Merck 0.2 mm silica gel 60 F-254 Al-plates. ¹H and ¹³C NMR spectra were obtained using Bruker DRX-500 Avance spectrometers. The powder X-ray diffraction pattern was recorded using a X-PERT-PRO diffractometer with Cu K α , ($\lambda = 1.54 \text{ \AA}$) irradiation, in the range of 5 to 80 (2θ) with a scan step of 0.026. The morphology of catalyst was studied with scanning electron microscopy using SEM (AIS2300C SEI) on gold-coated samples. Elemental analysis of the nanocomposite was provided by TESCAN-VEGA II energy-dispersive X-ray (EDX) analysis.

Preparation of $\gamma\text{-Fe}_2\text{O}_3\text{@cellulose-OSO}_3\text{H}$

At first, the cellulose microcrystal (5.00 g) was added to 20 mL of CHCl_3 and stirred vigorously. Then, 1.00 g of chlorosulfonic acid diluted in 5 mL of chloroform was added dropwise at 0 °C during 2 h. When the addition was completed,

the mixture was stirred for 2 h until HCl was removed from reaction vessel. Finally, the mixture was filtered and washed with methanol (3*10 mL) and dried at room temperature to afford cellulose sulfuric acid. In second, an aqueous solution of NaOH, urea, and H₂O was prepared with material ratios 7:12:81, respectively. Then, the temperature was decreased to -12 °C by use of ice and salt (NaCl). After that, 2.0 g of the synthesized cellulose sulfuric acid was added. Next, 0.5 g of FeCl₂.4H₂O and 1.0 g of FeCl₃. 6H₂O were dissolved in 50 mL of deionized water and added dropwise to the cellulose sulfuric acid solution. Finally, the resulted mixture was filtered and washed with water, ethanol and acetone and dried at room temperature to afford γ -Fe₂O₃ nanoparticles coated on cellulose sulfuric acid as a brown composite powder.

General procedure for the synthesis of pyranopyrazole derivatives

A mixture of an aldehyde **1** (1 mmol), malononitrile **2** (1 mmol), ethylacetoacetate **3** (1 mmol), hydrazine hydrate **4** (1 mmol), and γ -Fe₂O₃@cellulose-OSO₃H (0.005 g) in 2 mL of ethanol was vigorously stirred in a 5 mL round bottom flask at room temperature. The reaction progress was monitored by TLC. After completion of the reaction, the catalyst was separated by an external magnet. The pure products were obtained by recrystallization from ethanol.

General procedure for the synthesis of spiro[indoline-3,4'-pyrano[2,3-c]pyrazole] derivatives

A mixture of isatin **1** (1 mmol), malononitrile or ethylcyanoacetate **6** (1 mmol), ethyl acetoacetate **7** (1 mmol), hydrazine hydrate (1 mmol), and γ -Fe₂O₃@cellulose-OSO₃H (0.01 g) in 2 mL of ethanol was stirred vigorously in a 5 mL round bottom flask at room temperature. Reaction progression was monitored by TLC. The reaction progress was monitored by TLC. After completion of the reaction, the catalyst was separated by an external magnet. The catalyst was washed by hot ethanol, dried and reused in subsequent reactions. The pure products were obtained by recrystallization from ethanol.

Spectral data

Cellulose microcrystalline

IR (KBr) cm⁻¹: 3338, 2898, 1656, 1429, 1369, 1163, 1110, 1058, 667, 615.

Cellulose-OSO₃H

IR (KBr) cm⁻¹: 3350, 2900, 1645, 1429, 1371, 1163, 1110, 1058, 667, 613, 561.

γ -Fe₂O₃@cellulose-OSO₃H

IR (KBr) cm⁻¹: 3353, 2894, 1633, 1423, 1367, 1201, 1155, 1062, 1027, 663, 565, 437.

6-Amino-3,4-dimethyl-4-(4-nitrophenyl)-2,4-dihydropyran-2,3-c]pyrazole-5-carbonitrile (Table 2, Entry 27)

White powders (94%): mp 193–195 °C. IR (KBr) cm⁻¹: 3481, 3223, 3122, 2189, 1641, 1596, 1490, 1470, 1352. ¹H NMR (500.13 MHz, DMSO-*d*₆) δ : 1.7 (3H, s, CH₃), 1.7 (3H, s, CH₃), 6.9 (2H, br s, NH₂), 7.5 (2H, d, *J* = 8.9 Hz, H-Ar), 8.1 (2H, d, *J* = 8.9 Hz, H-Ar), 12.1 (1H, s, NH).

6-Amino-4-(4-methoxy-3-(phenoxyethyl)phenyl)-3-methyl-2,4-dihydropyran-2,3-c]pyrazole-5-carbonitrile (Table 2, Entry 24)

White powders (94%): mp 189–191 °C. ¹H NMR (500.13 MHz, DMSO-*d*₆) δ : 1.7 (3H, s, CH₃), 3.7 (3H, s, OCH₃), 4.5 (1H, s, CH), 5.0 (2H, s, CH₂), 6.8–7.4 (10H, m, H-Ar and NH₂). 12.065 (1H, s, NH). ¹³C NMR (125.61 MHz, DMSO-*d*₆) δ : 9.7, 35.7, 39.5, 55.5, 57.3, 69.9, 97.6, 111.9, 113.21, 120.0, 127.9, 128.3, 135.6, 136.8, 137.0, 147.3, 148.0, 154.7, 160.7.

6'-Amino-5-chloro-3'-methyl-5'-propionyl-2'H-spiro[indoline-3,4'-pyrano[2,3-c]pyrazol]-2-one (Table 5, Entry 10)

White powder (92%); mp 280–282 °C; IR (KBr) cm⁻¹: 3417, 3311, 3240, 1695, 1666, 1475, 1292, 1199. ¹H NMR (500.13 MHz, DMSO-*d*₆) δ : 0.7 (3H, t, *J* = 7.1 Hz, CH₃), 1.6 (3H, s, CH₃), 3.6–3.8 (2H, m, CH₂), 6.8 (1H, d, *J* = 8.2 Hz, H-Ar), 6.8 (1H, d, *J* = 1.8 Hz, H-Ar), 7.1 (1H, dd, *J* = 5.1 and 2.1 Hz, H-Ar), 8.0 (2H, br s, NH₂), 10.5 (1H, s, NH), 12.2 (1H, s, NH).

Acknowledgements The authors gratefully acknowledge partial support from the Research Council of the Iran University of Science and Technology.

References

1. A. Maleki, Ultrason. Sonochem. **40**, 460 (2018)
2. A. Maleki, Tetrahedron **68**, 7827 (2012)
3. A. Maleki, R. Firouzi-Haji, Z. Hajizadeh, Int. J. Biol. Macromol. **116**, 320 (2018)
4. H.M. Al-Matar, K.D. Khalil, A.Y. Adam, M.H. Elnagdi, Molecules **15**, 6619 (2010)
5. Z.H. Ismail, G.M. Aly, M.S. El-Degwi, H.I. Heiba, M.M. Ghorab, Egypt. J. Biotechnol. **13**, 73 (2003)
6. M.E. Zaki, H.A. Soliman, O.A. Hiekal, A.E. Rashad, Z. Naturforsch. C. **61**, 1 (2006)

7. R. Moosavi-Zare, M.A. Zolfigol, E. Noroozizadeh, M. Tavasoli, V. Khakyzadeh, A. Zare, *New J. Chem.* **37**, 4089 (2013)
8. A. Maleki, A.A. Jafari, S. Yousefi, *Carbohydr. Polym.* **175**, 409 (2017)
9. A. Maleki, M. Ghassemi, R. Firouzi Haji, *Pure Appl. Chem.* **90**, 387 (2018)
10. A. Maleki, R. Ghalavand, R. Firouzi-Haji, *Iran. J. Catal.* **8**, 221 (2018)
11. A. Maleki, *Polycycl. Aromat. Compd.* **38**, 402 (2018)
12. G.S. Kumar, C. Kurumurthy, B. Veeraswamy, P.S. Rao, P.S. Rao, B. Narsaiah, *Org. Prep. Proced. Int.* **45**, 429 (2013)
13. J. Ebrahimi, A. Mohammadi, V. Pakjoo, E. Bahramzade, A. Habibi, *J. Chem. Sci.* **124**, 1013 (2012)
14. H. Mecadon, M.R. Rohman, M. Rajbangshi, B. Myrboh, *Tetrahedron Lett.* **52**, 2523 (2011)
15. R.J. Sundberg, *Indoles*. (Academic Press, New York, 1996)
16. J.F. Da Silva, S.J. Garden, A.C. Pinto, *J. Braz. Chem. Soc.* **12**, 273 (2001)
17. K.C. Joshi, P. Chand, *Pharmazie* **37**, 1 (1982)
18. K.C. Joshi, R. Jain, K. Sharma, S.K. Bhattacharya, R.K. Goel, *J. Indian Chem. Soc.* **115**, 202 (1988)
19. A.H. Abdel-Rahman, E.M. Keshk, M.A. Hanna, S.M. El-Bady, *Bioorg. Med. Chem.* **12**, 2483 (2004)
20. A. Maleki, *Helv. Chim. Acta* **97**, 587 (2014)
21. A. Maleki, *Tetrahedron Lett.* **54**, 2055 (2013)
22. A. Maleki, A.A. Jafari, S. Yousefi, V. Eskandarpour, *C.R. Chim.* **18**, 1307 (2015)
23. A. Maleki, V. Eskandarpour, J. Rahimi, N. Hamidi, *Carbohydr. Polym.* **208**, 251 (2019)
24. A. Maleki, A.A. Jafarim, S. Yousefi, *J. Iran. Chem. Soc.* **14**, 1801 (2017)
25. A. Maleki, M. Aghaei, R. Paydar, *J. Iran. Chem. Soc.* **14**, 485 (2017)
26. Z. Hajizadeh, A. Maleki, *Mol. Catal.* **460**, 87 (2018)
27. H.V. Chavan, S.B. Babar, R.U. Hoval, B.P. Bandgar, *Bull. Korean Chem. Soc.* **32**, 3963 (2011)
28. K. Kanagaraj, K. Pitchumani, *Tetrahedron Lett.* **51**, 3312 (2010)
29. S.N. Darandale, J.N. Sangshetti, D.B. Shinde, *J. Korean Chem. Soc.* **56**, 328 (2012)
30. M.A. Nasser, S.M. Sadeghzadeh, *Monatsh. Chem.* **144**, 151 (2013)
31. K. Ablajan, W. Liju, A. Tuoheti, Y. Kelimu, *Lett. Org. Chem.* **9**, 639 (2012)
32. P.P. Bora, M. Bihani, G. Bez, *J. Mol. Catal. B* **92**, 24 (2013)
33. Y.M. Litvinov, A.A. Shestopalov, L.A. Rodinovskaya, A.M. Shestopalov, *J. Comb. Chem.* **11**, 914 (2009)
34. M. G. Dekamin, M. Alikhani, A. Emami, H. Ghafuri and S. Javanshir, *J. Iran. Chem. Soc.*, 2016, 13, 591.
35. Y. Zou, Y. Hu, H. Liu, D. Shi, *ACS Comb. Sci.* **14**, 38 (2011)
36. R.G. Redkin, L.A. Shemchuk, V.P. Chernykh, O.V. Shishkin, S.V. Shishkina, *Tetrahedron* **63**, 11444 (2007)
37. R.Y. Guo, Z.M. An, L.P. Mo, S.T. Yang, H.X. Liu, S.X. Wang, Z.H. Zhang, *Tetrahedron* **69**, 9931 (2013)
38. J. Feng, K. Ablajan, A. Sali, *Tetrahedron* **70**, 484 (2014)
39. S. Ahadi, Z. Yasaei, A. Bazgir, *Heterocycl. Chem.* **47**, 109 (2010)
40. K. Ablajan, L.J. Wang, Z. Maimaiti, Y.T. Lu, *Monatsh. Chem.* **145**, 491 (2014)
41. H. Sachdeva, R. Saroj, *Sci. World J.*, (2013). <https://doi.org/10.1155/2013/680671>